Nucleic Acids Research, Vol. 20, No. 11 2627–2637

How are tRNAs and mRNA arranged in the ribosome? An attempt to correlate the stereochemistry of the tRNA-mRNA interaction with constraints imposed by the ribosomal topography

Valery Lim, Česlovas Venclovas, Alexander Spirin, Richard Brimacombe[1]*, Philip Mitchell[1] and Florian Müller[1]
Institute of Protein Research, Russian Academy of Sciences, Pushchino, Moscow Region 142292, Russia and [1]Max-Planck-Institut für Molekulare Genetik, Abteilung Wittmann, Ihnestrasse 73, 1000 Berlin 33, Germany

Received April 10, 1992; Accepted May 6, 1992

ABSTRACT

Two tRNA molecules at the ribosomal A- and P-sites, with a relatively small angle between the planes of the L-shaped molecules, can be arranged in two mutually exclusive orientations. In one (the 'R'-configuration), the T-loop of the A-site tRNA faces the D-loop of the P-site tRNA, whereas in the other (the 'S'-configuration) the D-loop of the A-site tRNA faces the T-loop of the P-site tRNA. A number of stereochemical arguments, based on the crystal structure of 'free' tRNA, favour the R-configuration. In the ribosome, the CCA-ends of the tRNA molecules are 'fixed' at the base of the central protuberance (the peptidyl transferase centre) of the 50S subunit, and the anticodon loops lie in the neck region (the decoding site) of the 30S subunit. The translocation step is essentially a rotational movement of the tRNA from the A- to the P-site, and there is convincing evidence that the A-site must be located nearest to the L7/L12 protuberance of the 50S subunit. The mRNA in the two codon-anticodon duplexes lies on the 'inside' of the 'elbows' of the tRNA molecules (in both the S-type and R-type configurations), and runs up between the two molecules from the A- to the P-site in the 3' to 5'-direction. These considerations have the consequence that in the S-configuration the mRNA in the codon-anticodon duplexes is directed towards the 50S subunit, whereas in the R-configuration it is directed towards the 30S subunit. The results of site-directed cross-linking experiments, in particular cross-links to mRNA at positions within or very close to the codons interacting with A- or P-site tRNA, favour the latter situation. This conclusion is in direct contradiction to other current models for the arrangement of mRNA and tRNA on the ribosome.

INTRODUCTION

During the process of peptide chain elongation on the ribosome, aminoacyl tRNA is bound to the ribosomal A-site and peptidyl tRNA to the P-site. Transpeptidation occurs by attack of the amino group of the aminoacyl-tRNA on the ester group of the peptidyl-tRNA, resulting in a transfer of the peptide chain—prolonged by one amino acid residue—to the A-site bound tRNA. Translocation of the mRNA-tRNA-peptide complex then takes place, so that the peptidyl tRNA moves from the A- to the P-site, and the 'empty' tRNA from the P- to the E-site (e.g. 1–6). A number of intermediate states are most probably also involved in these processes (e.g. 7,8).

At the moment of transpeptidation the A- and P-site bound tRNAs are conformationally tightly constrained by the concomitant requirements for the respective CCA-termini to be drawn together in order to allow formation of the peptide bond, and at the same time for their anticodon loops to make contact with adjacent codons on the mRNA. The translocation event can be considered as a rotational movement of the A-site bound tRNA into the P-site, about an axis—the 'translocation axis' (9)—joining the CCA-termini and anticodon loops. The constrained stereochemistry at the A- and P-sites has aroused a great deal of interest, and a number of detailed stereochemical models have been proposed for the interaction between two tRNA molecules and a segment of mRNA in this configuration (e.g. 10–15). A variety of models (with or without mRNA) have also been suggested for the arrangement of the A-site and P-site bound tRNA molecules on the ribosome (e.g. 16–19, 8), but few attempts have so far been made to correlate and combine the two types of model-building study. In this article we attempt to make such a correlation, in order to narrow down the number of possible arrangements which satisfy both the detailed stereochemical requirements of the tRNA-mRNA interaction, and the topographical restrictions for the location of the two tRNAs and the mRNA on the ribosome.

* To whom correspondence should be addressed

We begin by describing the stereochemistry of two tRNA molecules at the A- and P-sites, and the way in which the orientation of these two tRNAs influences the path of the mRNA in the neighbourhood of the decoding site. (The E-site tRNA is not sufficiently constrained to be considered at this stage.) Next, we describe the evidence defining the positions of the two ends of the translocation axis on the 30S and 50S subunits, as well as the relative locations of the A- and P-sites in the ribosome. Published models which in one way or another are not compatible with these locations are discussed. Finally, we outline the evidence from 'site-directed cross-linking' studies with both tRNA and mRNA, which have the potential to discriminate between the various possible orientations. The conclusion we reach is that, while the question has yet to be finally settled, the evidence so far available supports a model which differs from those currently in vogue (e.g. 8,14,19).

I. MUTUAL ARRANGEMENT OF TWO tRNA MOLECULES AND mRNA

General stereochemical considerations

For simplicity we designate the two sides of the L-shaped tRNA molecule as the 'D' side and the 'T' side, according to the locations of the dihydrouridine and TΨC loops, respectively (cf. Fig. 1, below). As already mentioned above, at the A- and P-sites the two CCA-termini of the tRNAs are close together, and the two anticodon loops must base-pair with adjacent codons on the mRNA; the axis connecting the anticodons of the two tRNAs and their acceptor ends is defined as the translocation axis. The dihedral angle between the planes of the tRNAs is symbolized as 'w', and we define w = 0° when the tRNA planes are oriented in parallel, with the T-side of the A-site tRNA facing the D-side of the P-site tRNA. When the tRNA planes are coplanar, but with the 'elbows' drawn apart in opposite directions, then w = 180°. When w = 360° then the tRNA planes will again be parallel, but now with the D-side of the A-site tRNA facing the T-side of the P-site tRNA. The following discussion is based on a refinement of the stereochemical analysis originally made by Spirin & Lim (11). The refined analysis was made using the programme 'Frodo' to model the tRNA and/or mRNA on an Evans and Sutherland PS 390 computer graphics system, and simplified models (in which the phosphate backbone of the nucleic acid is represented by a 'tube') were generated on a VAX 8000 work station. Examples of the latter type of model are illustrated in Figure 1 below, with the more detailed Frodo representations of the codon-anticodon regions being shown in Figure 2.

In considering the mutual orientations of the two tRNA molecules, it must be emphasized that we use the stereochemistry for the anticodon loops and for the rest of the tRNA molecules as determined by crystallographic studies (20–22), and we make no serious distortions of this crystal structure. The validity of this assumption may have to be challenged at a later stage; it has for example already been demonstrated that significant differences occur in the configurations of both the CCA-terminus and the anticodon loop of tRNA in the crystal structure of the tRNA-synthetase complex (23,24) as opposed to the crystal structure of 'free' tRNA. However, in the absence of any specific evidence relating to the conformation of tRNA bound to the ribosome, the crystal structure of 'free' tRNA (20–22) remains the logical option for a stereochemical discussion of this nature.

The 'R' and 'S' configurations

Using the crystallographic structure, the parallel orientation with w = 0° (or up to 45°) is physically impossible, because the distance between the two anticodons in this orientation (10–20 Å) is greater than the maximal admissible distance between adjacent nucleotide residues (9 Å for a fully extended conformation). It follows that the possible configurations of the two tRNA molecules can be grouped into three classes. The first is the approximately perpendicular orientation with w = 90° (±45°) which was proposed by Rich (25) and analysed in detail by Spirin & Lim (11); this will be referred to as the *'R'-type orientation* (Fig. 1a, 2a). The second is also an approximately perpendicular orientation with w = 270° (±45°), which was proposed and analysed by Sundaralingam et al (10); this is designated the *'S-type' orientation* (Fig. 1b, 2b), and it is distinct

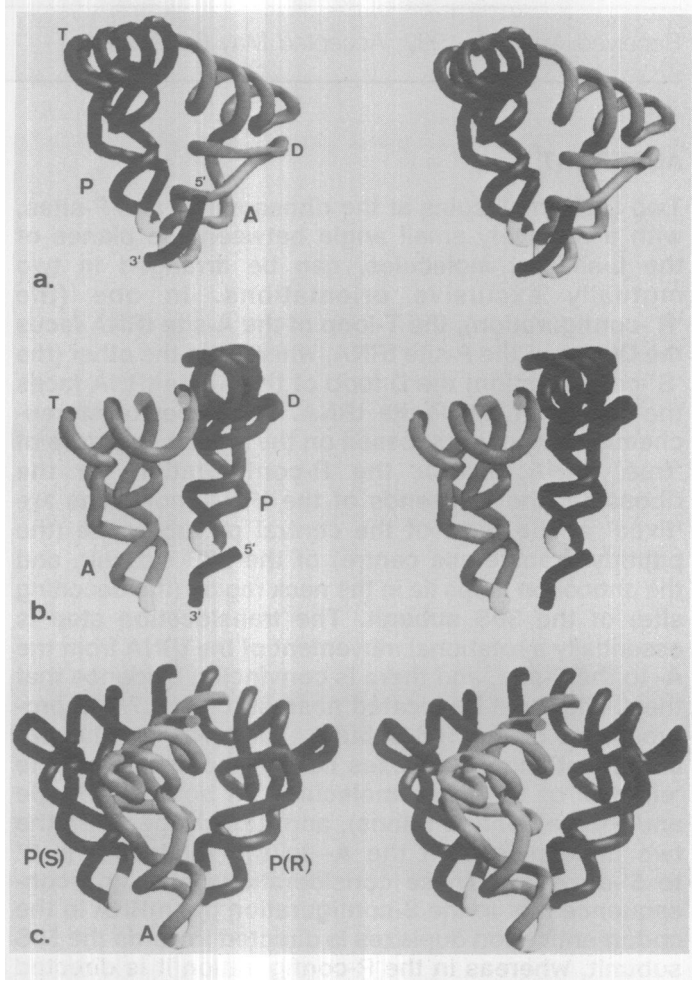

Figure 1. Mutual orientation of tRNA and mRNA molecules (stereo views). The phosphate backbones of the tRNA molecules are depicted (A-site tRNA lighter, P-site darker), with the anticodon regions in white. **a.** A-site and P-site tRNA in the R-configuration. The two interacting codons of mRNA are included (as phosphate backbones, in black), with the 5′ and 3′-ends indicated. 'D' and 'T' mark the dihydrouridine and TΨC loops, respectively, of the tRNA. **b.** A-site and P-site tRNA in the S-configuration, together with the two interacting codons of mRNA. Symbols as in 'a'. **c.** Comparison of the two alternative configurations (without mRNA). 'P(R)' indicates the position of a P-site tRNA in the R-orientation, 'P(S)' the corresponding position in the S-orientation, relative to a common A-site tRNA. (The view is from the opposite side of the tRNAs as compared with 'a' and 'b').

from and not superimposable on the R-configuration. A similar version of the same S-type orientation (in which the D-side of the A-site tRNA faces the T-side of the P-site tRNA) was also proposed by Mcdonald & Rein (12) and more recently by Nagano et al (15). The third class comprises the intermediate approximately coplanar orientations with w = 180° (±45°) or with w = 360° (or up to −45°).

Clearly, any experimental information about mutual effects of the two tRNAs on each other would be very helpful in discriminating between these theoretical possibilities. Unfortunately, such information is scarce, but there is one set of data which is directly pertinent to the problem. This is the measurement of singlet-singlet energy transfer between fluorescent probes attached to A- and P-site bound tRNA molecules on the ribosome (26,27). The former publication (26) showed that the distance between S^4U8-conjugated fluorescent dyes in the two tRNAs is about 30 Å or less, whereas the latter (27) evaluated the distance between the D-loops of the two tRNAs as being about 35 Å. These distances are much too short to be compatible with the coplanar configurations (with w = 180° or 360°), and the coplanar configurations will therefore not be considered further here. This leaves the R- and S-type orientations as the two possible candidates. However, the energy transfer measurements do not discriminate between the latter.

Detailed stereochemical arguments

Data from a further set of fluorescence measurements indicate that the D-loop of A-site bound tRNA—but not P-site bound tRNA—is affected by ribosomal residues, resulting in its immobilization (28). Other approaches have also implied that the D-loop participates in the interaction of tRNA with the A-site of the ribosome (29). In the case of the S-type orientation the D-loop of A-site bound tRNA faces the P-site bound tRNA, and thus the presence of ribosomal residues between the two tRNAs seems unlikely and would furthermore represent an obstacle for the translocational movement of tRNA from A- to P-site. This consideration therefore favours the R-type orientation, where the D-loop of A-site bound tRNA contacts the ribosomal surface and its T-loop faces the P-site bound tRNA (cf. Fig. 1).

In an entirely different type of study, Smith and Yarus (14) have shown that there is a strong influence of specific point mutations in the anticodon loop of the P-site tRNA on the codon-binding properties of the A-site tRNA. Changes on the 5′-side of the anticodon were especially effective, in particular when the conserved pyrimidine nucleotides (at positions 32 and 33) were substituted by purines. A weaker, but still significant effect was also observed in the case of loop substitutions on the 3′-side of the anticodon in the P-site tRNA. The authors concluded that the 5′-side of the anticodon loop of the P-site tRNA is in direct physical contact with the A-site tRNA, so that the substitution of pyrimidines by purines at these positions results in partial occlusion of the A-site. In other words, the P-site tRNA anticodon loop seems to form one 'wall' of the A-site in the ribosome. (Incidentally, this would explain the fact that the A-site cannot be occupied without previous occupation of the P-site (30−32,7)).

The crystallographic data (20−22) indicate that the conserved U-33 residue of the anticodon loop is involved in several interactions with the anticodon residues, including hydrogen bonding of its NH-group to the phosphate of residue 36 and the stacking of its pyrimidine ring with the phosphate of residue 35. Therefore, substitution of U-33 with other nucleotides—especially purine residues—must result in rearrangements of the sugar-phosphate backbone in the region of the 33rd residue. In our stereochemical analysis, it is the R-orientation of the two tRNAs (Fig. 2a) which provides the direct steric contact of this region of the P-site tRNA with the anticodon of the A-site tRNA (especially residue 36) and hence its plausible indirect influence, via the neighbouring residue 34 of the P-site tRNA, on the A-site codon. This is attained without any deformation of the crystallographic structure of the anticodons (Fig. 2a).

In contrast, however, Smith & Yarus (14), while also referring to the Rich model, in fact presented diagrams with the two tRNAs in the S-orientation. In the 'classical' S-orientation (10,12,15), the two anticodon loops are quite far apart from one another (see also Figs. 1b, 2b), and Smith & Yarus (14) were only able to draw the anticodon loops together in their model at the expense of some distortions of the anticodon loop structures, and by assuming a flexibility of the CCA-termini. In the stereo models (Figs. 4 and 5 of ref. 14) a local steric contact of residue 33 of the P-site tRNA is achieved with the sugar-phosphate backbone between the 38th and 39th residues of the A-site tRNA, rather than with the anticodon itself. Furthermore, strong steric overlaps arise between the sugar-phosphate backbone of the 34th and 35th residues of the P-site anticodon on the one hand, and the ribose rings of the 37th and 38th residues of the A-site tRNA on the other. Thus, the data of Smith & Yarus (14) can be accomodated in the R-configuration without distortion of the crystal structure

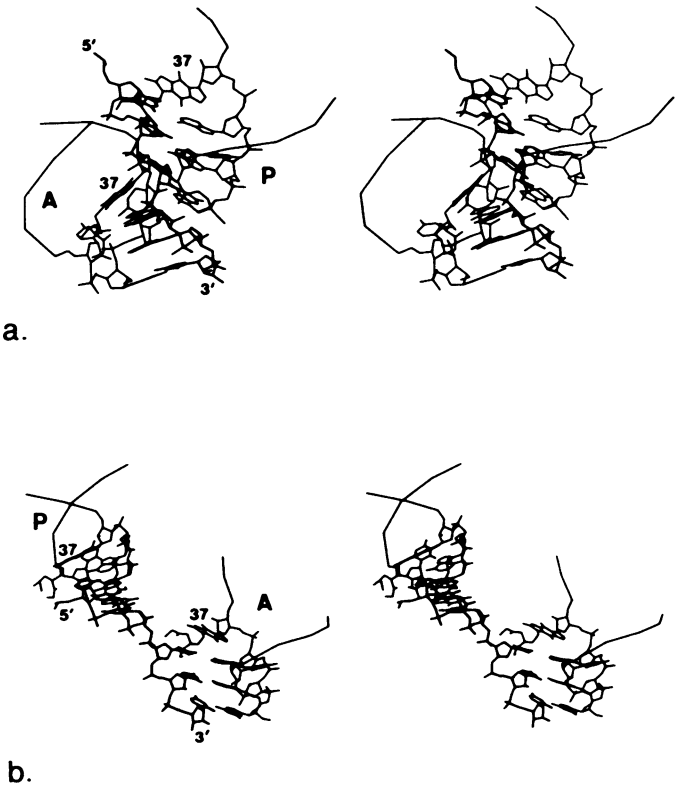

Figure 2. Details of the codon-anticodon interactions (stereo views). The two interacting codons of mRNA are shown in heavier lines (with 5′ and 3′-ends indicated), together with bases 33 to 37 (i.e. with one extra base on either side of the anticodon triplet) of both P-site and A-site tRNA molecules. Base 37 (marked) is depicted as a wybutine in all cases. **a.** The R-configuration. **b.** The S-configuration. (The view in both configurations is approximately the same as that in Figure 1c.)

(20–22), but can also be fitted to the S-configuration if suitable alterations are made to the latter.

Two further points should be mentioned here. In the case of the S-orientation the intercodon region of the mRNA is extended (Fig. 2b), thus making the A-site codon-anticodon duplex sensitive to distortions ('wobbles') at the third base of the P-site codon. This rigid connection between the two codon-anticodon duplexes is especially marked in the model of Smith & Yarus (14); most non-canonical base-pairings between the third base of the P-site codon and its anti-codon cannot be realized without disturbance of the A-site codon-anticodon duplex. On the other hand, due to the 'curved' conformation of the intercodon region in the case of the R-orientation (Fig. 2a), the third base of the P-site codon can form non-canonical (wobble) pairs with its anticodon without affecting the A-site codon-anticodon duplex.

The second consideration is based on the well-known fact of the absence of wobble in the pairing of the first and second bases of the A-site codon with its tRNA anticodon. This is not trivial, because wobble might be expected to occur at both ends of the codon-anticodon duplex. Stereochemical analysis of the R-orientation suggests that the sugar-phosphate moiety of the 5′-nucleotide of the A-site codon can be stacked on the wobble base pair of the P-site codon-anticodon duplex. Such a stacking interaction could create steric limitations preventing the formation of non-canonical base pairs in the first and second positions of the A-site codon.

Clearly, none of these considerations is thus far sufficient to formally exclude one or other of the tRNA arrangements. Most important, however, is the fact—which is overlooked by a surprising number of ribosomologists—that there are indeed two distinct possible orientations (R-type and S-type), and a glance at Figure 1c should convince the reader that these two configurations are non-superimposable and mutually exclusive.

The arrangement of mRNA relative to tRNA

For the modelling of the mRNA it is reasonable to allow two important assumptions: (1) All codon-anticodon duplexes exist as RNA A-form helices, with eleven base pairs per turn, and (2) the A-site codon-anticodon duplex and the corresponding P-site duplex are positioned relative to each other in a universal manner, which is independent of the tRNA species involved. In other words, the conformation of the internucleotide region between the A-site and P-site codons must be equivalent for all possible tRNA pairs. Furthermore, the two adjacent codon-anticodon duplexes cannot exist as a continuous coaxial helix, but there must be a 'kink' between them. This is apparent for the following reasons.

First, if the two codon-anticodon duplexes were stacked into a single A-form helix, then the acceptor ends of the two tRNA molecules would be forced apart. Secondly, it is sterically difficult to stack the A-site anticodon onto that of the P-site without serious deformation of the anticodon loop structures, because the 3′-base of the anticodon is already stacked onto the neighbouring base 37 in the anticodon loop. Thirdly, if (for example) yeast $tRNA^{Phe}$—which has the massive wybutine base at position 37—is placed in the A-site, then a coaxial or near-coaxial accomodation of the two codon-anticodon duplexes becomes impossible without a complete rearrangement of the anticodon loop structures. (In Figure 2 the tRNA anticodon loops are shown with a wybutine base at position 37). An interesting contribution to this question was made by Prabahakaran & Harvey (13), who conducted a stereochemical analysis of the extent to which the anticodon loops have to be distorted in order to accomodate an uninterrupted A-helix of the two adjacent mRNA codons.

It is also worth noting that the kink between two codons may be preserved both during and after translocation. In this case, the mRNA will also be kinked on the 5′-side of the P-site codon. Such a situation is consistent with the strong steric constraint already mentioned when a tRNA carrying a wybutine base at position 37 is involved, but now at the P- rather than the A-site; the mRNA cannot emerge from the P-site codon-anticodon duplex in the 5′-direction coaxially with the preceding duplex. Hence, in addition to the intercodon kink, it is likely that there is also a kink on the exit side of the P-site codon-anticodon helix (cf. Fig. 2a).

An important consequence of the stereochemistry of the mRNA in the codon-anticodon duplex for both R- and S-configurations (Fig. 2) is that in the 5′-direction the mRNA emerges on the 'inside' of the L-shapes of the A- and P-site tRNAs. If the mRNA were to pass out *between* the two tRNA molecules towards the 'outsides' of the L-shapes, then the movement involved in the translocation step would be impossible, because the tRNA would have to 'pass through' the mRNA chain during its rotation from the A- to the P-site. This is independent of any distortions of the anticodon loops which might in fact be present (cf. the foregoing discussion). Furthermore, it should be noted that in both configurations the A-site anticodon lies 'below' that of the P-site (Fig. 1), so that the general path of the mRNA is 'up between' the two tRNA molecules (see also Fig. 4, below), rather than 'across the base' of the anticodon loops as is so often depicted in cartoons of the functioning ribosome. Both these factors have decisive consequences for the placement of tRNA and mRNA in the ribosome.

II. THE ORIENTATION OF THE tRNA-mRNA COMPLEX IN THE RIBOSOME

The location of the translocation axis

The interpretations of electron microscopic images of ribosomes and their subunits made by various research groups (e.g. 33–39) have evolved to the point where there is a consensus of agreement between the different models, although there are still significant differences between them. The most detailed and objective description of the ribosome structure has been provided by the image processing (40) and three-dimensional image reconstruction techniques (41–43), and these results are taken here as the structural basis for considering the problem of tRNA and mRNA orientation. Particularly important in this context is the very recent three-dimensional reconstruction of unstained 70S ribosomes in amorphous ice (44).

The main features of the refined structure in relation to the older models are the very constricted neck of the small subunit, and the 'interface canyon' of the large subunit. It is also noteworthy that the 'platform' of the small subunit appears to be less pronounced and not so flat as in the model of Lake and his group (36,45), and we therefore prefer to use the term 'side lobe' rather than 'platform' for this feature. Furthermore, the area of direct structural contact between the two subunits in the 70S ribosome appears to be much less than was previously supposed, and this area is limited to relatively small regions on the L1 side of the 50S subunit and on the body of the 30S subunit. Thus the surfaces of both subunits, including parts of their 'interface sides', appear to be highly exposed to the solvent. In particular, the large area between the L7/L12 stalk and the central

protuberance of the 50S subunit is not covered by the 30S subunit and—together with the concave side surface of the 30S subunit—forms an open pocket or cavity which could accomodate large ligands such as tRNAs or elongation factors (cf. Fig. 5, below). Similarly, the 'interface side' of the head of the 30S subunit is located largely between the L1 protuberance and the central protuberance, so that it is also not fully covered by the opposing subunit. Schematic contour representations of both the small (30S) and large (50S) subunits, as well as the so-called 'overlap projection' of the complete (70S) ribosome, are given in Figure 3.

As already discussed, the ends of the translocation axis of tRNA molecules located at the A- and P-sites are defined by their anticodon loops on the one hand and their CCA-termini on the other. Strong evidence for the location of these features on the ribosome has been provided by immuno electron microscopy, foot-printing studies and chemical cross-linking experiments. These localizations have been confirmed by different techniques and various research groups, and the data can be summarized as follows.

The anticodons of the tRNAs (and thus the codons of the mRNA base-paired to them) are located on the 30S subunit of the translating ribosome, in the 'cleft' separating the head, body and side lobe regions (i.e. at the neck, see Fig. 3). An immediate contact between the 5'-base of the P-site tRNA anticodon and position C-1400 of the 16S RNA has been demonstrated by ultraviolet cross-linking (46), and this position has been localized in the cleft between the head and the side lobe by immuno electron microscopy (47). Model-building studies (48,49) show that the 16S RNA can be arranged in such a way as to accomodate this positioning. On the other hand it should be noted that in the electron-microscopically derived model of Vasiliev (33,39), there is virtually no cleft at all in the 30S subunit—rather just a 'ledge'. In terms of this model the intepretation of the immune electron microscopy data of Gornicki et al (47) leads to a location of the C-1400 residue on the 'neck' of the subunit (50), at a position which is significantly further to the right than that shown ('AC') in Figure 3.

The acceptor ends of the tRNAs are located on the 50S subunit, and have been placed at the base of the central protuberance by a number of immuno electron microscopy studies of antibiotics or their analogues that are involved in the peptidyl transferase process (e.g. 51–54). This position lies in the interface canyon of Frank et al (43,44). In cross-linking studies, protein L27 has been identified as the target of cross-linking to the 3'-terminal adenosine of tRNA (19), and this protein also lies at the base of the central protuberance, as shown by immuno electron microscopy (e.g. 54). Wower et al (19) showed further that the 3'-terminal adenosine of P-site bound tRNA can be cross-linked to position G-1945 of the 23S RNA, whereas affinity analogues of the aminoacyl residue (55,56) were cross-linked to positions within the 'peptidyl transferase ring', which comprises positions 2057–2063, 2447–2455, 2496–2506, 2582–2588 and 2606–2611 (57). Model-building studies on the 23S RNA (58) place all these sites, as well as the foot-print sites of the acceptor ends of both P- and A-site bound tRNA (59) at the base of the central protuberance.

It is clear from these data that the translocation axis is oriented from the cleft region ('neck') of the 30S subunit to the base of the central protuberance of the 50S subunit. A further important piece of evidence in this context is the identification of an inter-RNA cross-link between the 16S and 23S RNA molecules in the 70S ribosome (60). This cross-link—which was also found using polysomes as the substrate for the cross-linking reaction—connects residues 1408–1411 of the 16S RNA with residues 1912–1920 of the 23S RNA, positions which are close to the C-1400 and G-1945 residues, respectively, as just discussed above. These regions of the 16S and 23S RNA molecules are thus clearly located on the interface sides of the respective subunits, and indeed in the three-dimensional reconstruction of Frank et al (44) a 'bridge' is described between the 30S and 50S subunits, which corresponds well with the likely location of this inter-RNA cross-link (cf. 48,58).

In Figure 3, the translocation axis is shown in the overlap projection of the 70S ribosome. In this projection, the 30S subunit

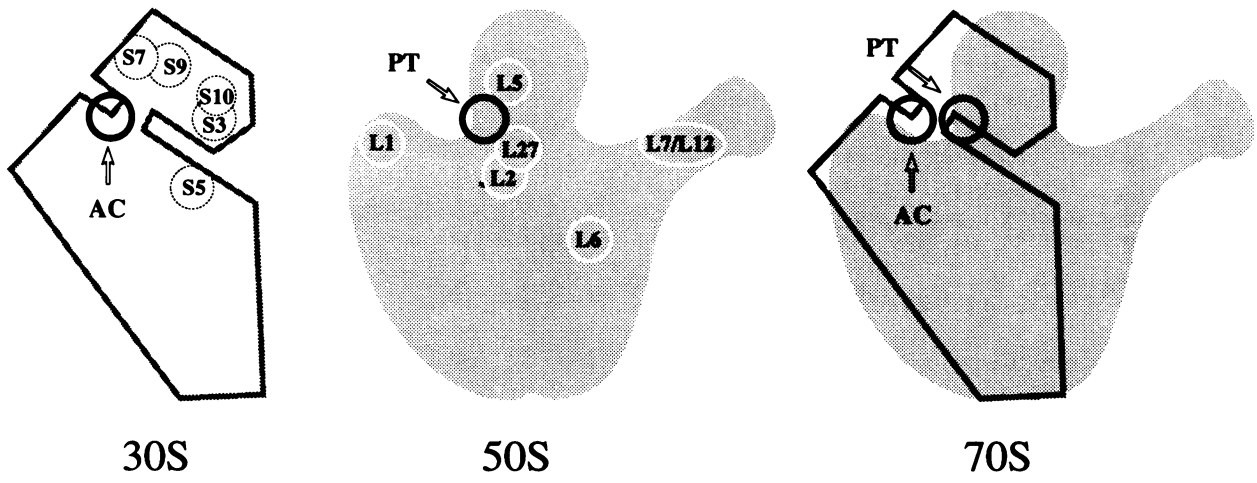

Figure 3. Orientation of the translocation axis in the ribosome. Schematic views of the 30S subunit, the 50S subunit, and the 70S ribosome (in the 'overlap' projection) are shown. The two ends of the translocation axis are denoted by 'AC' (for anticodon loop) and 'PT' (for peptidyl transferase centre), respectively. To avoid possible misinterpretation, it should be emphasized that both sites—AC and PT—lie on the interface side of their respective subunits. The positions of antigenic determinants of selected proteins are included for reference. See text for further explanation.

lies towards the viewer and is overlapped with the interface of the 50S subunit. The L1 ridge of the latter is on the left, and the L7/L12 stalk on the right, with the peptidyl transferase centre being obscured by the region of the 30S subunit near to the neck. The two ends of the translocation axis are indicated in Figure 3, although it must be borne in mind that the precise angle of this axis will depend on the detailed orientation of the two subunits relative to one another. In particular, using the model of Lake and his coworkers (45) the 'AC' end of the axis will be lower down (at the base of the deep cleft in that model), whereas using the model of Shatsky et al (50) the 'AC' end will lie to the right of the 'PT' end of the axis, as already noted above.

Since the extremities of the A- and P-site bound tRNAs are thus relatively firmly fixed by the two ends of the translocation axis, it follows that all possible positions of the two tRNAs can be described in terms of a rotation about this axis. However, the range of acceptable positions becomes severely restricted if one considers the question of the ribosomal elongation factors, in particular EF-Tu.

The location of elongation factor EF-Tu

Both elongation factors EF-Tu and EF-G bind to the ribosome in the region of the L7/L12 stalk and its base on the 50S subunit (61,62), and both show foot-prints in the highly conserved loop around position 2660 in the 23S RNA (63). Cleavage by α-sarcin within the latter loop prevents binding of the two factors (64). Cross-linking studies have shown that proteins L6 and L11 are neighbours of the elongation factors on the ribosome (e.g. 65–67), and these proteins are also located at the base of the L7/L12 stalk (54). It is well known that EF-Tu brings the aminoacyl tRNA to the A-site in the form of a ternary complex together with GTP, and when this complex is bound to the ribosome it gives a foot-print identical to that of tRNA in the A-site (68), at least in the case of 16S RNA. It should be noted that EF-Tu interacts with the outside of the acceptor limb, including the stem and TΨC-arm of the aminoacyl tRNA (e.g. 69–74); contacts with the D-arm (75) have not been confirmed by the rest of the available data.

From these data it follows that the A-site tRNA must be located on the L7/L12 side of the ribosome (relative to the P-site tRNA), as only in this case can serious perturbations of the tRNA contacts with the 16S RNA be avoided during EF-Tu release and A-site occupation (8). Thus, the possible rotation of the A- and P-site tRNAs about the translocation axis (see previous section) is limited to those positions where the A-site tRNA lies on the side of the L7/L12 stalk. In this context the foot-print data for E-site bound tRNA (76) are also important; the E-site foot-print lies predominantly within the RNA region which comprises the binding site for protein L1 (77), thus providing further evidence that the movement of tRNA from A- to P- to E-site runs in the direction from the L7/L12 protuberance towards the L1 protuberance.

In consequence, there are two general possible arrangements for the tRNA molecules at the A- and P-sites, and these are illustrated schematically in Figure 4, for the R-orientation (Fig. 4a) and the S-orientation (Fig. 4b), respectively. These two arrangements are clearly not interchangeable (a rotation about the translocation axis in Fig. 4a does not generate the configuration of Fig. 4b, and vice versa), and they reflect the different stereochemistries of the R- and S-configurations (Fig. 1). There is however considerable confusion in the literature on this point, with a number of authors claiming that their arrangement of tRNAs on the ribosome is 'consistent' with both the Rich and Sundaralingam orientations.

It is not clear at this stage how far the acceptor stems of the tRNA are 'buried' in the interface canyon (43), or how far the anticodon arms penetrate into the 30S subunit; the neck of the latter is as already mentioned very constricted, and the head is only joined to the body by a single helix (helix '28') of the 16S RNA (48,49), so there may be more space between head and body than the electron microscopy data suggest. There is of course also some degree of flexibility in the orientation of the translocation axis (see previous section) as well as in the angle of rotation of the two tRNAs about this axis. Nevertheless, if the A-site is indeed proximal to the L7/L12 stalk, then the available data only appear to allow the two basic arrangements of Figure 4, and—as already discussed—the stereochemical evidence favours the R-configuration, that is to say the arrangement of Figure 4a.

Published models for the arrangement of tRNA on the ribosome

The models that have been previously proposed for the orientation of two tRNA molecules (with or without mRNA) on the ribosome can be discussed in the light of the criteria considered above. The first model to be put forward was that of Lake (16). In this model, the anticodons of the A-site and P site tRNAs were placed in the cleft between the head and the side lobe of the 30S subunit, with the tRNA elbows on the left (in the orientation of Fig. 3) and the acceptor ends contacting the peptidyl transferase centre on the 50S subunit interface. The peptidyl transferase centre is rather far towards the L1-side in this model and the orientation of the two subunits is somewhat skewed in relation to the more recent proposals (43,44), but the most important feature of the Lake model is that both the A-site tRNA and the P-site tRNA are placed on the side of the 30S subunit farthest from the L7/L12 protuberance. In order to account for the interaction with EF-Tu on the L7/L12 side, the incoming tRNA must first bind to a presumed 'R-site' on the opposite side of the 30S subunit before 'flipping' round to the actual A-site. This suggestion is however not consistent with the observation of Moazed & Noller (68) that the foot-print on 16S RNA of A-site bound tRNA is identical to that of tRNA bound as a ternary complex, as already mentioned

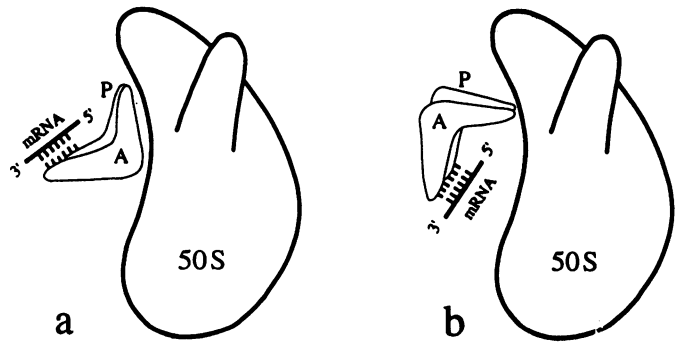

Figure 4. Schematic representation of the arrangement of two tRNA molecules together with mRNA on the 50S subunit. The L7/L12 stalk is towards the reader. The six bars on each mRNA denote two triplet codons, interacting with the A- and P-site tRNA anticodons. In 'a' the tRNA molecules are in the R-orientation, in 'b' in the S-orientation.

above. In the Lake model (16), the two tRNAs appear to be in the R-configuration.

An R-configuration is also used for the tRNA in the model proposed by Spirin (17). Here the tRNA pair was placed in the large cavity formed by the concave surface at the neck of the 30S subunit and the interface canyon of the 50S subunit. In contrast to the model of Lake, the acceptor ends are much closer to the L7/L12 stalk side of the 50S subunit. The anticodons were in the groove between the head and the body of the 30S subunit, i.e. in the neck region, in an orientation such that the C-1400 end of the translocation axis (see above) was reached from the right ('L7/L12') side of the neck (Fig. 3). As originally drawn by Spirin (17), this model does not appear to be consistent with the location of the C-1400 region on the interface side of the 30S subunit (60; see the discussion above). However, the general arrangement remains a possibility, if the neck of the subunit is indeed as highly constricted as the 16S RNA models (48,49) and the recent three-dimensional reconstruction from electron micrographs (44) would suggest.

A further example of the R-configuration is the model of Wagenknecht et al (42). In this case however the two tRNAs are rotated about the translocation axis (in relation to the arrangement of Figure 4a) so that the P-site tRNA is nearest to the L7/L12 stalk.

The S-orientation of the tRNAs is preferred in the models of refs. 8, 19, 49 and 78. Stern et al (49) proposed two alternative arrangements for two tRNA molecules in relation to the 30S subunit. In one of these (Figure 23 of that publication) the anticodon loops are located in the cleft of the 30S subunit, but the CCA-termini are pointing in a direction away from the 50S subunit; this arrangement can clearly be discounted. In the alternative proposal (Figure 24 of the publication) the CCA-termini reach the 50S subunit by leading around the solvent side of the 30S subunit in a manner similar to that proposed by Spirin (17) (see above). The more recent publications (8,19,78) propose essentially the arrangement of Figure 4b, with the elbows of the tRNAs pointing up and to the left (towards the 30S subunit). The location of the translocation axis, and the placing of the A-site tRNA towards the L7/L12 stalk, are consistent with the criteria discussed in the preceding sections, but—as is clear from Figure 4b—it is implicit in this arrangement that the mRNA runs up between the two tRNA molecules on the 50S side rather than on the 30S side (cf. Fig. 4a, and see below for further discussion).

An interesting contribution to the controversy concerning the S- versus R-orientation of the tRNAs was provided by the data of Ofengand et al (18). Here, photo-reactive labels attached to A-site bound tRNA at position 8, and to P-site bound tRNA at position 47 (in the latter case using a rather long reagent) both gave a cross-linking reaction with protein S19, which is located on the head of the 30S subunit. The authors argued in effect that their result favours the S-configuration (Figure 27.6 in that publication), because in this orientation position 8 of the A-site tRNA and position 47 of the P-site tRNA are facing towards each other, on the insides of the elbows of the two tRNA molecules (cf. Fig. 1). However, in order to accomodate this into a model for the arrangement of the tRNAs on the ribosome, Ofengand et al (18) were obliged to place the tRNAs with their CCA ends facing the 30S subunit rather than the 50S, and with the P-site closest to the L7/L12 stalk, thus violating two of the principal criteria discussed above.

The flaw in the argument—and at the same time the solution to the dilemma—lies in the implied assumption that the two cross-links to protein S19 are to the same point on the latter. Ribosomal proteins are not much smaller than the tRNA molecules themselves, and very little is known about their shapes and orientations in the ribosome. S19 in particular is a protein whose precise location on the head of the 30S subunit is in dispute (cf. 54,79,80). In the R-orientation, the two tRNA positions cross-linked to S19 (18) are about 40 Å apart, and in the arrangement of Figure 4a the insides of the tRNA elbows—where positions 8 and 47 are located—are facing towards the head of the 30S subunit. The data of Ofengand et al (18) are thus compatible with this R-configuration. (A similar arrangement to that of ref. 18, but with A-site tRNA only, was proposed by Olson et al (51).)

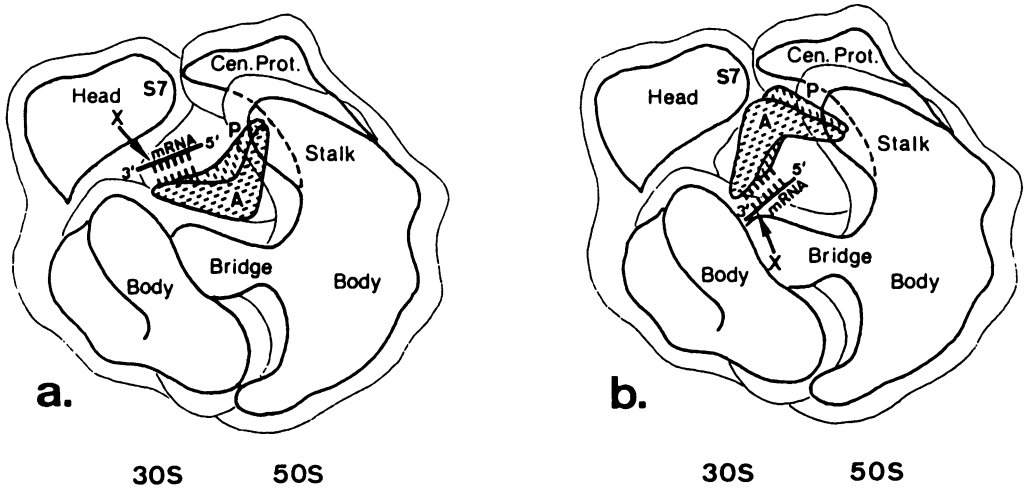

Figure 5. The mRNA-tRNA complex superimposed (approximately to scale) on the 70S ribosome model of Frank et al (44). The mRNA and P- and A-site tRNAs are depicted as in Fig. 4, 'a' in the R-orientation and 'b' in the S-orientation (cf. 78). (In either case, some degree of rotation about the translocation axis is allowable—see text.) The 30S subunit is on the left, with the position of protein S7 indicated (see text). The 50S subunit is on the right, 'Cen. Prot.' denoting the central protuberance of the latter. 'X' indicates the cross-link (94) to the 3'-base of the A-site codon of the mRNA.

The problem in the interpretation of the cross-links to S19 is a general one, which applies to all of the considerable body of chemical cross-linking data to ribosomal proteins which is accumulating for both tRNA and mRNA on the ribosome; the finite size of the ribosomal proteins, coupled with the uncertainty as to their precise locations in the ribosomal subunits as well as the length of the cross-linking reagents used, all have the effect of reducing the ability of a particular cross-link to discriminate between one model for the tRNA-mRNA arrangement and another. Nevertheless, some conclusions can be drawn, which are discussed in the following sections. For this purpose, the two basic tRNA-mRNA arrangements of Figure 4 are shown schematically superimposed on the 70S model of Frank et al (44) in Figure 5.

Chemical cross-linking to tRNA

The results of tRNA-ribosome cross-linking experiments have been recently reviewed in detail by Wower & Zimmermann (78), and include both 'site-directed' cross-linking data and data from direct UV-induced cross-linking (81–83). In the site-directed cross-linking method, a photo-reactive label is attached to a specified position of the tRNA and then allowed to react with the ribosome. Examples of this technique have already been discussed in the preceding sections, including the cross-links to the 3'-terminus of tRNA (19) (which help to define the orientation of the translocation axis) and the cross-links to protein S19 from P-site or A-site bound tRNA (18). In similar experiments, Podkowinski & Gornicki (84) attached a probe to position 37 in the anticodon loop of P-site bound tRNA, and identified cross-links to proteins S7 and L1. The same authors (85) also identified L33 as the target of cross-linking to a probe attached at position 20 in the D-loop of P-site tRNA. According to the protein map of Walleczek et al (86) L33 lies between proteins L27 (at the base of the central protuberance of the 50S subunit) and L1. These results are consistent with both arrangements for the tRNA illustrated in Figures 4 and 5, but do not discriminate between them. Similarly, the finding (18) that position C-1400 of the 16S RNA can be cross-linked to the anticodon loops of both A- and P-site bound tRNA does not discriminate between the two models. On the other hand, the cross-links from the anticodon loop to proteins S7 and L1 (84)—albeit using a rather long probe—speak against the model of Shatsky et al (50), in which (as already discussed) the anticodon loop end of the translocation axis is located further towards the L7/L12 stalk (Fig. 3).

A further data set which should be mentioned in this connection are the measurements of Hardesty et al (87,88), who used singlet-singlet energy transfer to determine the distance between proteins S21 and L11 (cf. 54) and different parts of the P-site tRNA. The distance between S21 and a S^4U-8 coupled label on the tRNA was reported to be 63–90 Å, whereas that between the same protein and the anticodon loop was somewhat shorter (45–64 Å). The corresponding distance from protein L1 to the S^4U-8 label was 65–84 Å. Again, however, these measurements are consistent with both basic tRNA arrangements (Fig. 5).

The results obtained by direct UV-cross-linking are less easy to interpret (81–83). Cross-links in the A-site to S10 (position 9 of the tRNA), L27 (position 18), S7 (position 26) and L2 (position 59) fit better with the arrangement of Figure 5a than with that of Figure 5b (cf. Fig. 3). On the other hand, the corresponding set of cross-links in the P-site (L2, position 17 of the tRNA; S7, position 45; S5, position 21; L5, position 44; L27, position 56; S9, position 60) show a distribution of agreements and disagreements with both arrangements.

The surprising fact in this data set is that closely neighboured residues on the same surface of the tRNA, particularly in the P-site, can apparently interact with such remote proteins as S5, L5 and S7, even when using the 'zero-length' UV-cross-linking method. This could reflect the fact that the ribosome is certainly not a rigid structure, and its various domains may undergo significant movement even within a defined functional state; evidence for this has already begun to accumulate from other cross-linking studies (89). Alternatively, it could reflect a heterogeneity of binding of the tRNA to the various ribosomal sites. Further studies—in particular using the 'site-directed cross-linking' method under controlled conditions—should help to resolve this problem.

The path of mRNA through the ribosome

The configuration of the mRNA is obviously tightly constrained in the immediate vicinity of the decoding site by the corresponding configurations of the A- and P-site bound tRNAs (Fig. 2). From the two model arrangements shown in Figures 4 and 5 it can be seen that in the S-configuration (Fig. 4b, 5b) the mRNA lies on the side of the tRNA anticodon loops facing the 50S rather than the 30S subunit. In the R-configuration (Fig. 4a, 5a), the reverse is true, which is consistent with the fact that cross-linking to the mRNA at positions close to the decoding site is exclusively to the 30S subunit (see below). In the arrangement of Wower & Zimmermann (78)—which is essentially that of Figures 4b and 5b, and which uses the 'Lake' models for the ribosomal subunits—the tRNAs are placed in a position such that the 'platform' of the 30S subunit intervenes between the anticodon loops of the tRNAs and the 50S subunit; although this would appear to enable the mRNA to contact the 30S subunit (on the inside of the 'platform') rather than the 50S subunit, it is difficult to realize such an arrangement in a detailed model of the structure (our unpublished observations). It should further be noted that this placement of the 'platform' (78) precludes any significant penetration of the acceptor stems of the tRNAs into the interface canyon of the 50S subunit (43,44). Again, therefore, the R-configuration (Fig. 4a, 5a) appears to be the preferred one, and detailed results from site-directed cross-linking studies with mRNA at positions close to the decoding site provide further support for this arrangement.

Olson et al (90) have shown by immuno electron microscopy that the 'anti-Shine–Dalgarno' sequence at the extreme 3'-terminus of the 16S RNA is located on the side lobe of the 30S subunit in an orientation which suggests strongly that the 'outgoing' or 5'-side of the mRNA leaves the ribosome from the cleft in a 'northerly' direction (cf. 91). Using the site-directed cross-linking technique, Stade et al (92) confirmed this by demonstrating that at positions on the mRNA on the 5'-side of the P-site codon, cross-linking occurred exclusively to ribosomal protein S7 and to the 3'-terminal 30 bases of the 16S RNA. The same cross-links were observed in several positions on the mRNA, one being only two nucleotides away from the 5'-base of the P-site codon. This result is clearly consistent with the R-configuration (Fig. 5a), in which the anticodon loops are directed towards the cleft of the 30S subunit, with the 5'-side of the mRNA lying close to the position of protein S7 on the head of the 30S subunit (cf. Fig. 3). The 3'-terminal region of the 16S RNA—which is known to be rather flexible (e.g. 48)—can also be readily

reached from this position. On the other hand, it is difficult to imagine how a position on the mRNA only two bases away from the P-site codon could reach protein S7 in the S-configuration (Fig. 5b, and ref. 78); in the latter arrangement this position on the mRNA must lie deep down on the inside of the side lobe of the 30S subunit, with the anticodon loops of the tRNAs (cf. Fig. 2b) intervening between the mRNA and the head of the subunit (and hence S7).

In the case of the 'incoming' or 3'-side of the mRNA, there are essentially two possibilities. The mRNA can either approach the decoding site from the interface side of the 30S subunit, or it can approach from the solvent side by passing round the back of the neck. However, since as already discussed, the head of the 30S subunit is only connected to the body by a single helix (helix 28; ref. 48), this question becomes reduced to the question of whether the mRNA passes 'to the left' or 'to the right' of this helix (cf. Fig. 3), and the resolution of the available data is not yet sufficient to answer this. It is furthermore not unlikely that the approaching mRNA may be actually 'buried' between the head and the body of the 30S subunit; this could offer a mechanism for the by no means trivial task of unfolding large secondary structural elements of the mRNA as they approach the decoding site.

The R-type orientation of the two tRNAs (Fig. 5a) is suggestive of an arrangement whereby the mRNA approaches from the solvent side of the 30S subunit by passing through the neck region, and the site-directed cross-linking data so far available lend support to this idea. At positions in the mRNA close to the 3'-side of the coding triplet, Rinke-Appel et al (93) found cross-links to protein S5, a protein which is located on the solvent side of the 30S subunit (79; cf. Fig. 3). At positions further away from the decoding site, S1 was cross-linked, again a protein which lies clearly on the solvent side of the subunit.

Most important, however, is a cross-link observed in the 30S initiation complex by Dontsova et al (94) from position +6 of the mRNA, i.e. from the 3'-base of the A-site coding triplet. This cross-link was entirely dependent on the presence of $tRNA^{fMet}$ at the P-site, and was to position ca 1050 of the 16S RNA; the same cross-link has since been observed in 70S ribosomes, and has been localized to position 1052 (Dontsova, Dokudovskaya, Kopylov, Bogdanov, Rinke-Appel, Jünke and Brimacombe, manuscript submitted). Nucleotide 1052 lies within 'helix 34' of the 16S RNA, and in both of the three-dimensional models for the latter (48,49) this helix is located within the head of the 30S subunit, by virtue of its position in the 3'-domain of the 16S secondary structure. The cross-link thus not only supports an approach of the 3'-side of the mRNA through the neck region from the solvent side of the subunit, but also provides further support for the R-configuration (Fig. 5a). In contrast, a cross-link from the 3'-base of the A-site codon to the 1050 region of the 16S RNA is unlikely with the S-configuration (Fig. 5b); in the latter configuration (cf. 78) the 3'-base of the A-site codon could contact the inside of the side lobe or the body of the 30S subunit, but not the head of the latter. However, as already mentioned above, there is some flexibility in the orientation of the translocation axis, and also in the angle of rotation of the two tRNAs about this axis in the model arrangements of Figures 4 and 5. Furthermore, it should be noted that the precise positioning of helix 34 within the head of the 30S subunit (48, cf. 49), as well as the locations of other regions of the 16S RNA model, are currently undergoing revision in our laboratory. Thus, although the tRNA-mRNA arrangement of Figure 5a appears to be the most plausible, a modified version of the S-configuration in relation to that depicted in Fig. 5b and refs. 8, 78 cannot be entirely excluded at this stage.

An approach of the mRNA from the solvent side through the neck region is reminiscent of the mRNA arrangement proposed by Gold (95), in which the mRNA lies in a channel along the solvent side of the 30S subunit. Further support for this type of arrangement comes from the observation (96) that the 'toe-print' of mRNA as determined by a reverse transcriptase assay of the 3'-region of ribosome-bound mRNA is identical for 30S-mRNA and 70S-mRNA complexes. The arrangement is attractive, because it keeps the bulky elements of the translation machinery segregated from one another. Thus, tRNA and elongation factors approach via the 30S-50S interface region, the mRNA approaches from the solvent side, and the nascent peptide goes out through a groove or tunnel (e.g. 97–100) in the 50S subunit.

CONCLUSIONS

1. The question of the arrangement of tRNA and mRNA on the ribosome can only be effectively studied if all the components involved, *viz.* tRNA, mRNA and both ribosomal subunits, are considered together as a single entity.

2. There are two mutually exclusive basic configurations of the A-site and P-site bound tRNA, namely the R- and the S-configuration.

3. Both the stereochemical evidence for the mutual arrangement of the tRNAs and the results of topographical studies with the ribosome favour the R-configuration.

4. An approach of the 3'-side of the mRNA from the solvent side through the neck region of the 30S subunit, and an exit of the 5'-side of the mRNA upwards towards the head of the latter, are also favoured by both the stereochemical analysis (R-configuration) and the experimental (cross-linking) data presently available.

5. Further site-directed cross-linking experiments—in particular those involving cross-links to the ribosomal RNA—with both tRNA and mRNA, combined with refinements to the current three-dimensional models of the 16S and 23S RNA, have the potential of providing a definitive answer to these questions.

REFERENCES

1. Watson, J.D. (1964) *Bull. Soc. Chim. Biol.* **46**, 1399–1425.
2. Wettstein, F.O. and Noll, H. (1965) *J. Mol. Biol.* **11**, 35–53.
3. Rheinberger, H.J., Sternbach, H. and Nierhaus, K.H. (1981) *Proc. Natl. Acad. Sci. USA* **78**, 5310–5314.
4. Rheinberger, H.J., Geigenmüller, U., Gnirke, A., Hausner, T.P., Remme, J., Saruyama, H. and Nierhaus, K.H. (1990) In Hill, W.E., Dahlberg, A.E., Garrett, R.A., Moore, P.B., Schlessinger, D. and Warner, J. (eds), *The Ribosome; Structure, Function and Evolution*, ASM Press, Washington DC, pp 318–330.
5. Kirillov, S.V., Makarov, E.M. and Semenkov, Y.P. (1983) *FEBS Lett.* **157**, 91–94.
6. Wintermeyer, W., Lill, R. and Robertson, J. (1990) In Hill, W.E., Dahlberg, A.E., Garrett, R.A., Moore, P.B., Schlessinger, D. and Warner, J. (eds), *The Ribosome; Structure, Function and Evolution*, ASM Press, Washington DC, pp 348–357.
7. Wintermeyer, W. and Robertson, J. (1982) *Biochemistry* **21**, 2246–2252.
8. Noller, H.F., Moazed, D., Stern, S., Powers, T., Allen, P.N., Robertson, J.M., Weiser, B. and Triman, K. (1990) In Hill, W. E., Dahlberg, A.E., Garrett, R.A., Moore, P.B., Schlessinger, D. and Warner, J. (eds), *The Ribosome; Structure, Function and Evolution*, ASM Press, Washington DC, pp 73–92.

9. Spirin, A.S. (1985) *Progr. Nucleic Acid Res. and Mol. Biol.* **32**, 75–114.
10. Sundaralingam, M., Brennan, T., Yathindra, N. and Ichikawa, T. (1975) In Sundaralingam, M. and Rao, S.T. (eds), *Structure and Conformation of Nucleic Acids and Protein–Nucleic Acid Interactions*, University Park Press, Baltimore, pp 101–115.
11. Spirin, A.S. and Lim, V. (1986) In Hardesty, B. and Kramer, G. (eds), *Structure, Function and Genetics of Ribosomes*, Springer-Verlag, New York, pp 556–572.
12. McDonald, J.J. and Rein, R. (1987) *J. Biomolec. Struct. Dynamics* **4**, 729–744.
13. Prabahakaran, M. and Harvey, S.C. (1989) *J. Biomolec. Struct. Dynamics* **7**, 167–179.
14. Smith, D. and Yarus, M. (1989) *Proc. Natl. Acad. Sci. USA* **86**, 4397–4401.
15. Nagano, K., Takagi, H. and Harel, M. (1991) *Biochimie* **73**, 947–960.
16. Lake, J.A. (1977) *Proc. Natl. Acad. Sci. USA* **74**, 1903–1907.
17. Spirin, A.S. (1983) *FEBS Lett.* **156**, 217–221.
18. Ofengand, J., Ciesiolka, J., Denman, R. and Nurse, K. (1986) In Hardesty, B. and Kramer, G. (eds) *Structure, Function and Genetics of Ribosomes*, Springer-Verlag, New York, pp 473–494.
19. Wower, J., Hixson, S.S. and Zimmermann, R.A. (1989) *Proc. Natl. Acad. Sci. USA* **86**, 5232–5236.
20. Kim, S.H., Suddath, F.L., Quigley, G.J., McPherson, A., Sussman, J.L., Wang, A.H.J., Seeman, N.C. and Rich, A. (1974) *Science* **185**, 435–440.
21. Robertus, J.D., Ladner, J.E., Finch, J.T., Rhodes, D., Brown, R.S., Clark, B.F.C. and Klug, A. (1974) *Nature* **250**, 546–551.
22. Moras, D., Comarmond, M.B., Fischer, J., Weiss, R., Thierry, J.C., Ebel, J.P. and Giegé, R. (1980) *Nature* **288**, 669–674.
23. Rould, M.A., Perona, J.J., Söll, D. and Steitz, T.A. (1989) *Science* **246**, 1135–1142.
24. Ruff, M., Krishnaswamy, S., Boeglin, M., Poterszman, A., Mitschler, A., Podjarny, A., Rees, B., Thierry, J.C. and Moras, D. (1991) *Science* **252**, 1682–1689.
25. Rich, A. (1974) In Nomura, M., Tissières, A. and Lengyel, P. (eds), *Ribosomes*, Cold Spring Harbor Press, New York, pp 871–884.
26. Johnson, A.E., Adkins, H.J., Matthews, E.A. and Cantor, C.R. (1982) *J. Mol. Biol.* **156**, 113–140.
27. Paulsen, H., Robertson, H.J. and Wintermeyer, W. (1983) *J. Mol. Biol.* **167**, 411–426.
28. Robertson, J.M. and Wintermeyer, W. (1981) *J. Mol. Biol.* **151**, 57–79.
29. Sprinzl, M., Wagner, T., Lorenz, S. and Erdmann, V.A. (1976) *Biochemistry* **15**, 3031–3039.
30. De Groot, N., Panet, A. and Lapidot, Y. (1971) *Eur. J. Biochem.* **23**, 523–527.
31. Lührmann, R., Eckhardt, H. and Stöffler, G. (1979) *Nature* **280**, 423–425.
32. Wurmbach, P. and Nierhaus, K.H. (1979) *Proc. Natl. Acad. Sci. USA* **76**, 2143–2147.
33. Vasiliev, V.D. (1974) *Acta Biol. Med. Germ.* **33**, 779–793.
34. Tischendorf, G.W., Zeichhardt, H. and Stöffler, G. (1974) *Mol. Gen. Genet.* **134**, 187–208.
35. Tischendorf, G., Zeichhardt, H. and Stöffler, G. (1975) *Proc. Natl. Acad. Sci. USA* **72**, 4820–4824.
36. Lake, J.A. (1976) *J. Mol. Biol* **105**, 131–159.
37. Boublik, M., Hellmann, W. and Roth, H.E. (1976) *J. Mol. Biol.* **107**, 479–490.
38. Boublik, M., Hellmann, W. and Kleinschmidt, A.K. (1977) *Cytobiologia* **14**, 293–300.
39. Vasiliev, V.D., Selivanova, O.M., Baranov, V.I. and Spirin, A.S. (1983) *FEBS Lett.* **155**, 167–172.
40. Van Heel, M. and Stöffler-Meilicke, M. (1985) *EMBO J.* **4**, 2389–2395.
41. Frank, J., Radermacher, M., Wagenknecht, T. and Verschoor, A. (1988) *Methods Enzymol.* **164**, 3–35.
42. Wagenknecht, T., Carazo, J.M., Radermacher, M. and Frank, J. (1989) *Biophys. J.* **55**, 455–464.
43. Frank, J., Verschoor, A., Radermacher, M. and Wagenknecht, T. (1990) In Hill, W.E., Dahlberg, A.E., Garrett, R.A., Moore, P.B., Schlessinger, D. and Warner, J., (eds), *The Ribosome; Structure, Function and Evolution*, ASM Press, Washington, DC, pp 107–113.
44. Frank, J., Penczek, P., Grassucci, R. and Srivastava, S. (1991) *J. Cell Biol.* **115**, 597–605.
45. Oakes, M., Henderson, E., Scheinman, A., Clark, M. and Lake, J.A. (1986) In Hardesty, B. and Kramer, G., (eds), *Structure, Function and Genetics of Ribosomes*, Springer-Verlag, New York, pp 47–67.
46. Prince, J.B., Taylor, B.H., Thurlow, D.L., Ofengand, J. and Zimmermann, R.A. (1982) *Proc. Natl. Acad. Sci. USA* **79**, 5450–5454.
47. Gornicki, P., Nurse, K., Hellmann, W., Boublik, M. and Ofengand, J. (1984) *J. Biol. Chem.* **259**, 10493–10498.
48. Brimacombe, R., Atmadja, J., Stiege, W. and Schüler, D. (1988) *J. Mol. Biol.* **199**, 115–136.
49. Stern, S., Weiser, B. and Noller, H. F.. (1988) *J. Mol. Biol.* **204**, 447–481.
50. Shatsky, I.N., Bakin, A.V., Bogdanov, A.A. and Vasiliev, V.D. (1991) *Biochimie* **73**, 937–945.
51. Olson, H.M., Grant, P.G., Cooperman, B.S. and Glitz, D.G. (1982) *J. Biol. Chem.* **257**, 2649–2656.
52. Olson, H.M., Nicholson, A.W., Cooperman, B.S. and Glitz, D.G. (1985) *J. Biol. Chem.* **260**, 10326–10331.
53. Stöffler, G. and Stöffler-Meilicke, M. (1984) *Ann. Rev. Biophys. Bioeng.* **13**, 303–330.
54. Stöffler, G. and Stöffler-Meilicke, M. (1986) In Hardesty, B. and Kramer, G. (eds), *Structure, Function and Genetics of Ribosomes*, Springer-Verlag, New York, pp 28–46.
55. Barta, A., Steiner, G., Brosius, J., Noller, H.F. and Kuechler, E. (1984) *Proc. Natl. Acad. Sci. USA* **81**, 3607–3611.
56. Steiner, G., Kuechler, E. and Barta, A. (1988) *EMBO J.* **7**, 3949–3955.
57. Vester, B. and Garrett, R.A. (1988) *EMBO J.* **7**, 3577–3587.
58. Mitchell, P., Osswald, M., Schüler, D. and Brimacombe, R. (1990) *Nucleic Acids Res.* **18**, 4325–4333.
59. Moazed, D. and Noller, H.F. (1991) *Proc. Natl. Acad. Sci. USA* **88**, 3725–3728.
60. Mitchell, P., Osswald, M. and Brimacombe, R. (1992) *Biochemistry* **31**, 3004–3011.
61. Girshovich, A.S., Kurtskhalia, T.V., Ovchinnikov, V.A. and Vasiliev, V.D. (1981) *FEBS Lett.* **130**, 54–59.
62. Girshovich, A.S., Bochkareva, E.S. and Vasiliev, V.D. (1986) *FEBS Lett.* **197**, 192–198.
63. Moazed, D., Robertson, J.M. and Noller, H.F. (1988) *Nature* **334**, 362–364.
64. Hausner, T.P., Atmadja, J. and Nierhaus, K.H. (1987) *Biochimie* **69**, 911–913.
65. Maassen, J.A. and Möller, W. (1978) *J. Biol. Chem.* **253**, 2777–2783.
66. Maassen, J.A. and Möller, W. (1981) *Eur. J. Biochem.* **115**, 279–285.
67. Sköld, S.E. (1982) *Eur. J. Biochem.* **127**, 225–229.
68. Moazed, D. and Noller, H.F. (1990) *J. Mol. Biol.* **211**, 135–145.
69. Boutorin, A.S., Clark, B.F.C., Ebel, J.P., Kruse, T.A., Petersen, H.U., Remy, P. and Vassilenko, S. (1981) *J. Mol. Biol.* **152**, 593–608.
70. Wikman, F.P., Siboska, G.E., Petersen, H.U. and Clark, B.F.C. (1982) *EMBO J.* **1**, 1095–1100.
71. Kao, T.H., Miller, D.L., Abo, M. and Ofengand, J. (1983) *J. Mol. Biol.* **166**, 383–405.
72. Joshi, R.L., Faulhammer, H., Chapeville, F., Sprinzl, M. and Haenni, A.L. (1984) *Nucleic Acids Res.* **12**, 7467–7478.
73. Gebhardt-Singh, E. and Sprinzl, M. (1986) *Nucleic Acids Res.* **14**, 7175–7188.
74. Kiesewetter, S., Ott, G. and Sprinzl, M. (1990) *Nucleic Acids Res.* **18**, 4677–4682.
75. Douthwaite, S., Garrett, R.A. and Wagner, R. (1983) *Eur. J. Biochem.* **131**, 261–269.
76. Moazed, D. and Noller, H.F. (1989) *Cell* **57**, 585–597.
77. Branlant, C., Korobko, V. and Ebel, J.P. (1976) *Eur. J. Biochem.* **70**, 471–482.
78. Wower, J. and Zimmermann, R.A. (1991) *Biochimie* **73**, 961–969.
79. Capel, M.S., Kjeldgaard, M., Engelman, D.M. and Moore, P.B. (1988) *J. Mol. Biol.* **200**, 65–87.
80. Olson, H.M., Olah, T.V., Cooperman, B.S. and Glitz, D.G. (1988) *J. Biol. Chem.* **263**, 4801–4806.
81. Abdurashidova, G.G., Tsvetkova, E.A. and Budowsky, E.I. (1989) *FEBS Lett.* **243**, 299–302.
82. Abdurashidova, G.G., Tsvetkova, E.A. and Budowsky, E.I. (1990) *FEBS Lett.* **269**, 398–401.
83. Abdurashidova, G.G., Tsvetkova, E.A. and Budowsky, E.I. (1991) *Nucleic Acids Res.* **19**, 1909–1915.
84. Podkowinski, J. and Gornicki, P. (1989) *Nucleic Acids Res.* **17**, 8767–8782.
85. Podkowinski, J. and Gornicki, P. (1991) *Nucleic Acids Res.* **19**, 801–808.
86. Walleczek, J., Schüler, D., Stöffler-Meilicke, M., Brimacombe, R. and Stöffler, G. (1988) *EMBO J.* **7**, 3571–3576.
87. Hardesty, B., Odom, O.W. and Deng, H.Y. (1986) In Hardesty, B. and Kramer, G. (eds), *Structure, Function and Genetics of Ribosomes*, Springer-Verlag, New York, pp 495–508.
88. Hardesty, B. Odom, O.W. and Czworkowski, J. (1990) In Hill, W.E., Dahlberg, A.E., Garrett, R.A., Moore, P.B., Schlessinger, D. and Warner,

J. (eds), *The Ribosome; Structure, Function and Evolution*, ASM Press, Washington DC, pp 366–372.
89. Doering, T., Greuer, B. and Brimacombe, R. (1991) *Nucleic Acids Res.* **19**, 3517–3524.
90. Olson, H.M., Lasater, L.S., Cann, P.A. and Glitz, D.G. (1988) *J. Biol. Chem.* **263**, 15196–15204.
91. Evstafieva, A., Shatsky, I.N., Bogdanov, A.A., Semenkov, Y. and Vasiliev, V.D. (1983) *EMBO J.* **2**, 799–804.
92. Stade, K., Rinke-Appel, J. and Brimacombe, R. (1989) *Nucleic Acids Res.* **17**, 9889–9908.
93. Rinke-Appel, J., Jünke, N., Stade, K. and Brimacombe, R. (1991) *EMBO J.* **10**, 2195–2202.
94. Dontsova, O., Kopylov, A. and Brimacombe, R. (1991) *EMBO J.* **10**, 2613–2620.
95. Gold, L. (1988) *Annu. Rev. Biochem.* **57**, 199–233.
96. Hartz, D., McPheeters, D.S. and Gold, L. (1990) In Hill, W. E. Dahlberg, A.E., Garrett, R.A., Moore, P.B., Schlessinger, D. and Warner, J. (eds), *The Ribosome; Structure, Function and Evolution*, ASM Press, Washington DC, pp 275–280.
97. Malkin, L.I. and Rich, A. (1967) *J. Mol. Biol.* **26**, 329–346.
98. Bernabeu, C. and Lake, J.A. (1982) *Proc. Natl. Acad. Sci. USA* **79**, 3111–3115.
99. Ryabova, L.A., Selivanova, O.M., Baranov, V.I., Vasiliev, V.D. and Spirin, A.S. (1988) *FEBS Lett.* **226**, 255–260.
100. Yonath, A., Bennett, W., Weinstein, S. and Wittmann, H.G. (1990) In Hill, W.E., Dahlberg, A.E., Garrett, R.A., Moore, P.B., Schlessinger, D. and Warner, J. (eds), *The Ribosome; Structure, Function and Evolution*, ASM Press, Washington DC, pp 134–147.